Construction and Building Materials 264 (2020) 120200

Contents lists available at ScienceDirect

Construction and Building Materials

journal homepage: www.elsevier.com/locate/conbuildmat

Effect of the fibre type on concrete impact resistance

J.C. Vivas [a], R. Zerbino [a,*], M.C. Torrijos [a], G. Giaccio [b]

[a] CONICET. LEMIT and Faculty of Engineering UNLP, La Plata, Argentina
[b] CIC. LEMIT and Faculty of Engineering UNLP, La Plata, Argentina

HIGHLIGHTS

- Impact behaviour of concretes with steel, polymer and glass fibres is analysed.
- Cracking and post-cracking responses were studied using drop-weight impact tests.
- The variation of cumulated energy with the crack opening differs with the fibre type.
- The crack opening growth rate allows to compare impact resistance of fibre concretes.
- Fibre type modifies the static residual stresses vs. impact resistance relationship.

ARTICLE INFO

Article history:
Received 18 December 2019
Received in revised form 26 June 2020
Accepted 8 July 2020

Keywords:
Crack control
FRC class
Impact
Glass macrofibres
Polymer macrofibres
Steel fibres

ABSTRACT

Fibre Reinforced Concrete performance is evaluated in terms of bending residual stresses. Although fibre concrete is suitable for structures exposed to impacts and other extreme loads, there is not much information about the relationship between the static residual capacity and the impact strength. Concretes incorporating steel, glass and polymer macrofibres were evaluated by means of a repeated drop-weight impact test. The cracking resistance and the post-cracking behaviour were compared. While the first crack mainly depends on the matrix strength, there is a direct relationship between static residual stresses and the impact resistance, but it varies with the type of fibre.

1. Introduction

Fibre Reinforced Concrete (FRC) is a high-performance material for both the construction and reinforcement of structural elements exposed to impacts and other types of extreme loads. Many studies refer the benefits of fibres incorporation in concretes exposed to explosions [1–4], ballistic shocks [5], cyclic loads [6], and different types of impact [7–9]. Numerous methods to evaluate the FRC impact resistance have been proposed, such as the oscillating pendulum (Charpy type) [10], pressure bar (Split-Hopkinson) [11], rotating machine [12], ACI committee 544 drop weight test [13], and other different drop-weight impact tests [14,15]. In the last report of ACI 544 committee [16], a description of available FRC impact tests is presented; they are classified in instrumented and non-instrumented. The formers include measure of load, displacement or acceleration, among other variables, during the impact time. Other important review can be find in [17]. However, there is no consensus about a method to characterize the impact response of FRC. In addition, and considering that many different types of fibres have been developed in the last years, fibre contribution to concrete impact resistance, especially in the cracked state, is of great interest.

Nowadays, many new fibres providing structural capacity are available, however, the literature review reflects that not much research compares the impact performance of concretes reinforced with different types of fibres. Most experiences were done with steel FRC.

Banthia et al. [18] compared the flexure impact resistance, through a simple drop-weight impact instrumented test, on plain concrete and on steel and polypropylene FRC. They found that 0.5% in volume of polypropylene fibres increased near 50% the fracture energy while 1.5% of steel fibres triplicated it. Bindiganavile et al. [19,20] studied FRC prepared with polymeric and steel fibres; they developed fibre–matrix bond impact tests and bending

* Corresponding author.
E-mail addresses: juancarlos.vivas@ext.ing.unlp.edu.ar (J.C. Vivas), zerbino@ing.unlp.edu.ar (R. Zerbino), mc.torrijos@conicet.gov.ar (M.C. Torrijos), ggiaccio@ing.unlp.edu.ar (G. Giaccio).

https://doi.org/10.1016/j.conbuildmat.2020.120200
0950-0618/

impact tests. The pull-out test showed that at high rates both fibres increased bond strength, but at very high velocities steel fibres (flat end) presented lower bond and energy absorption capacity than the polymeric fibres. Flexure impact tests showed similar trend. In another research [21] it was found that impact loads and higher loading rates enhance pull-out resistance of steel fibres in UHPC, however they also found that deformed steel fibres break easily than straight fibres under impact loads; the effectiveness of the loading rate on both the average bond strength and pull-out energy was higher for straight fibres, followed by half-hooked fibres, twisted fibres and finally hooked fibres. Yoo et al. [22] compared the impact behaviour of ultra-high performance concretes incorporating different steel fibres. While the first peak strength was not affected by fibres, the use of long straight steel fibres enhanced the post-cracking impact resistance when compared to short straight and twisted fibres; this was attributed to an increase in the number and branching of cracks. A study on impact capacity [23], using the tests proposed by the ACI committee 544, was performed on steel, polypropylene and cellulose FRC. It showed that cellulose fibres increased the first crack strength and that polypropylene fibres improved the post-crack behaviour.

There is a general consensus that FRC performance must be evaluated in terms of the residual capacity; in this way the *fib* Model Code 2010 [24] established FRC classes from the residual stresses determined using the EN14651 standard bending test [25]. Nevertheless, there is not much information about the relationship between the static residual capacity and the impact resistance.

In this paper the performance of concretes incorporating steel, glass and polymer macrofibres was evaluated by means of a repeated drop-weight impact test. The cracking resistance and the post-cracking behaviour were compared. The relationship between static residual stresses and the impact resistance is discussed.

2. Experimental program

2.1. Materials and mixtures

Seven concretes were done, one reference concrete (R) without fibres and six FRC, incorporating two different contents of steel (S), polymer (P), and glass (G) macrofibres. The FRC were identified as S25, S50, P5, P10, G6, and G12, where the letter corresponds to the type of fibre and the number indicates fibre content (in kg/m^3). The adopted fibre contents, corresponding to dosages used in many structural applications, were selected to obtain FRC covering a wide range of residual capacities. Table 1 and Fig. 1 show the characteristics of the used fibres.

All FRC were prepared using the same base concrete proportions (Concrete R). It incorporates 390 kg/m^3 of Portland cement, 880 kg/m^3 of natural siliceous sand, 845 kg/m^3 of 12 mm maximum size granitic crushed stone and 5.8 kg/m^3 of superplasticizer. When fibers were incorporated the dosage of superplasticizer was increased (between 1.5 and 2 %) in order to obtain a slump equal to 60 ± 10 mm. The water/cement ratio was 0.41 by weight.

Table 1
Characteristics of the fibres.

Designation	S	G	P
Type	Steel	Glass	Polymer
Shape	Hooked-end	Flat	Embossed
Length, l (mm)	50	36	58
Diameter, ϕ (mm)	1.00	0.54	0.67
Aspect ratio, l/ϕ	50	67	87
Tensile strength (MPa)	> 1100	> 1700	> 640
Elastic modulus (GPa)	210	72	6.8
Density (kg/m^3)	7850	2680	910

Six prisms of 150x150x600 mm and six cylinders of 100x200 mm were cast with each concrete. All specimens were consolidated by external vibration. They were cured in a moist room for 28 days (RH: 95%, temperature 23 °C) and then remained in laboratory indoor up to testing in order to minimize the variation of concrete mechanical properties during the testing period. EN14651 beams and cylinders for static characterization were tested at the age of three months, and after that impact tests were done.

2.2. Concrete mechanical properties

Compression and bending tests were carried out following ASTM C-39 [26] and EN14651 [25] standards respectively. Fig. 2 shows the average stress-crack mouth opening displacement (CMOD) curves of each concrete. Table 2 presents the mean values of compressive strength (f'_C), first crack, or limit of proportionality, stress (f_L) and the residual stresses f_{R1} and f_{R3} corresponding to CMOD of 0.5 and 2.5 mm respectively. Fig. 2 and Table 2 show that FRC with a wide range of toughness were studied varying f_{R1} between 1.8 and 5.4 MPa and f_{R3} between 0.9 and 4.9 MPa. Regarding the fibre type, it is also interesting to note that P10, G12 and S25 concretes have very similar f_{R1}.

2.3. Impact test

A repeated drop-weight test was implemented. In preliminary experiences different alternatives for loads application, geometry of the specimens, the variability of results, the minimum number of specimens required and different parameters to characterize the impact resistance were studied [27].

Fig. 3.a shows the impact testing device. It has two vertical steel rails to guide the hammer, which is elevated and positioned, manually or using an electric motor, at the desired height (up to 4 m). After the hammer reaches that height it is released, the drop occurs and impacts the specimen at the middle span. This type of equipment, available in many laboratories around the world, was originally designed for various drop-weight tests on steel specimens [28,29]. Fig. 3.b shows a detail of hammer adopted for this study, which has 5 kg-mass, 150 mm length and semi-circular section linear "Tup".

The device has two identical steel supports where prismatic specimens can be placed on (see Fig. 3.c). Each support has a metallic bar that fixes the sample and prevents lifting during and after each impact. On both supports the specimen rests on cylinders that allow the sample to rotate at the plane of impact. The distance between supports can also be varied as they rest on a rail system. It should be noted that the proposed methodology reproduces an isostatic system, one of the supports is fixed to the base while the other is left free (properly lubricated), so that it is allowed to move horizontally.

The impact tests were performed on prismatic 150x150x300 mm specimens, which were the twelve halves resulting from the static bending characterization test (EN14651). Before testing, a 25 mm depth notch was sawn at the centre of the tensile face. As was confirmed in a previous study, using this notch depth no shear failure occurs. The test procedure consists on repeated drops of a hammer (with a mass m) on the top of the specimen from a certain height (h). After each impact, the Crack Opening Displacement (COD) is measured at 120 mm below the top face of the prism. A Dino-Lite Premier digital microscope® AM4113T, 1.3 Megapixels, was used to measure the evolution of the cracks. An increased image of up to 250x is obtained and, with the provided

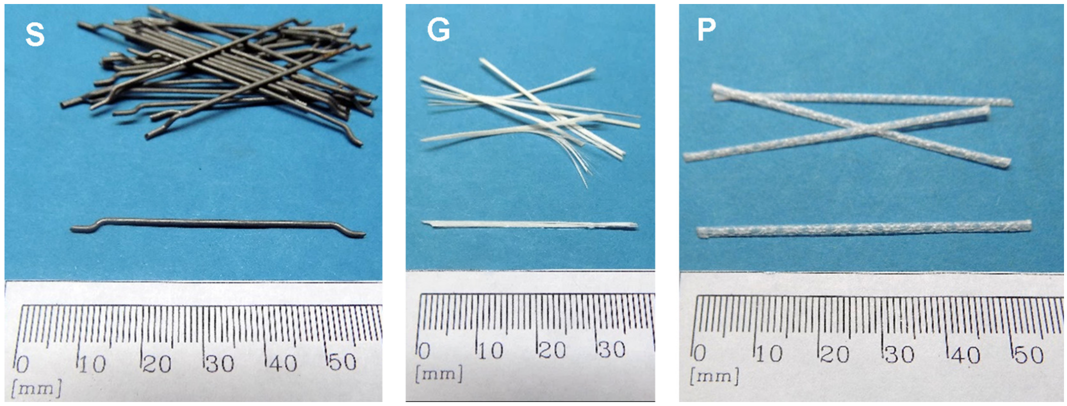

Fig. 1. Used fibres: (S) steel (G) glass and (P) polymeric.

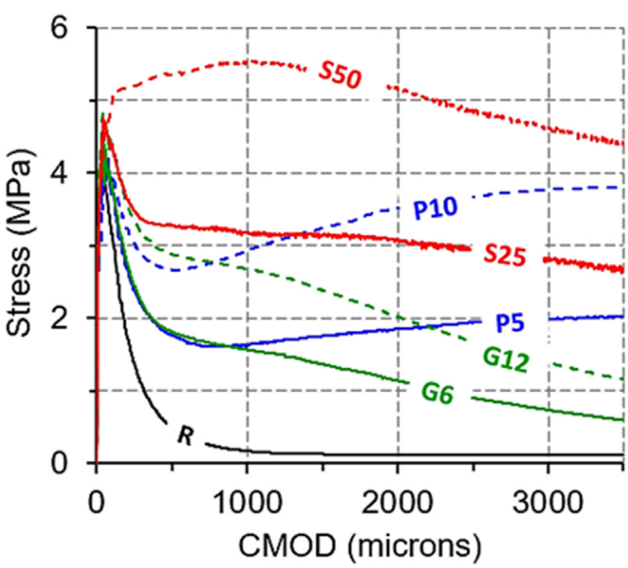

Fig. 2. Mean curves from characterization bending tests (EN 14651) [25].

software, it is possible to measure cracks with a precision of 0.0001 mm.

Table 3 shows the test protocol, which consists of two phases. The objective of the first phase is to determine the cracking resistance, while the second phase has the aim of evaluating the contribution of fibres in cracked state. In this way, in Phase 1 impact loads are applied on the sound specimen, while in Phase 2 they are applied after cracking. In both cases the drop height of the hammer is progressively increased. In Phase 1 the adopted initial height (h_0) was 100 mm, the height increments between consecutive impacts (Δh) were 50 mm, and only one drop was applied for each height level; the process finishes when a crack is detected (this crack width is called Initial Crack Opening COD_C). Then, Phase 2 starts, using h_0 equal to 100 mm and Δh 100 mm, but in this case three impacts are applied at each height level. The end of the test occurs when the COD is>3 mm.

The energy (E) of each impact is calculated as $m{\cdot}g{\cdot}h$ (being g the acceleration of gravity) and corresponds to the potential energy introduced to the system before starting the drop. Fig. 4 shows a scheme of an impact curve where the cumulated energy versus COD is plotted. The cumulated energy is the sum of the energy of all impacts received by the specimen up to a certain point. The cracking energy, E_C, is the energy cumulated until the first visible crack appears; the post cracking energy, E_P, is that cumulated between the start of cracking and the end of test, when COD achieves 3 mm. Finally, the total energy E_T is also calculated as sum of E_C + E_P. COD_C is the initial crack opening and V_C the COD growth rate during Phase 2 (post-cracking). V_C is calculated from the cumulated energy between crack openings 0.5 mm ($E_{0.5}$) and 2.5 mm ($E_{2.5}$); then, V_C = 2 mm/($E_{2.5}$−$E_{0.5}$), expressed in mm/J. Table 3 summarizes the impact parameters corresponding to Phases 1 and 2.

3. Results and analysis

With the aim of showing the test variability the individual impact curves of concretes R, S25, P10, and G12 (all FRC with

Table 2
Concrete mechanical properties. Static tests. Coefficient of variation in percentage between brackets.

Concrete	Fibres			f'_C	f_L	f_{R1}	f_{R3}
	Type	(kg/m^3)	(volume %)		(MPa)		
R	–	–	–	44.2 (5)	4.1 (10)	–	–
S25	Steel	25	0.32	44.5 (4)	4.8 (10)	3.5 (18)	3.2 (21)
S50		50	0.64	44.8 (5)	4.9 (7)	5.3 (10)	4.7 (10)
G6	Glass	6	0.22	47.1 (4)	4.7 (5)	1.8 (19)	0.9 (22)
G12		12	0.44	46.6 (5)	4.9 (4)	2.9 (11)	1.7 (11)
P5	Polymer	5	0.55	47.3 (14)	4.5 (15)	1.8 (8)	1.9 (18)
P10		10	1.10	46.3 (4)	4.4 (4)	2.7 (12)	3.8 (18)

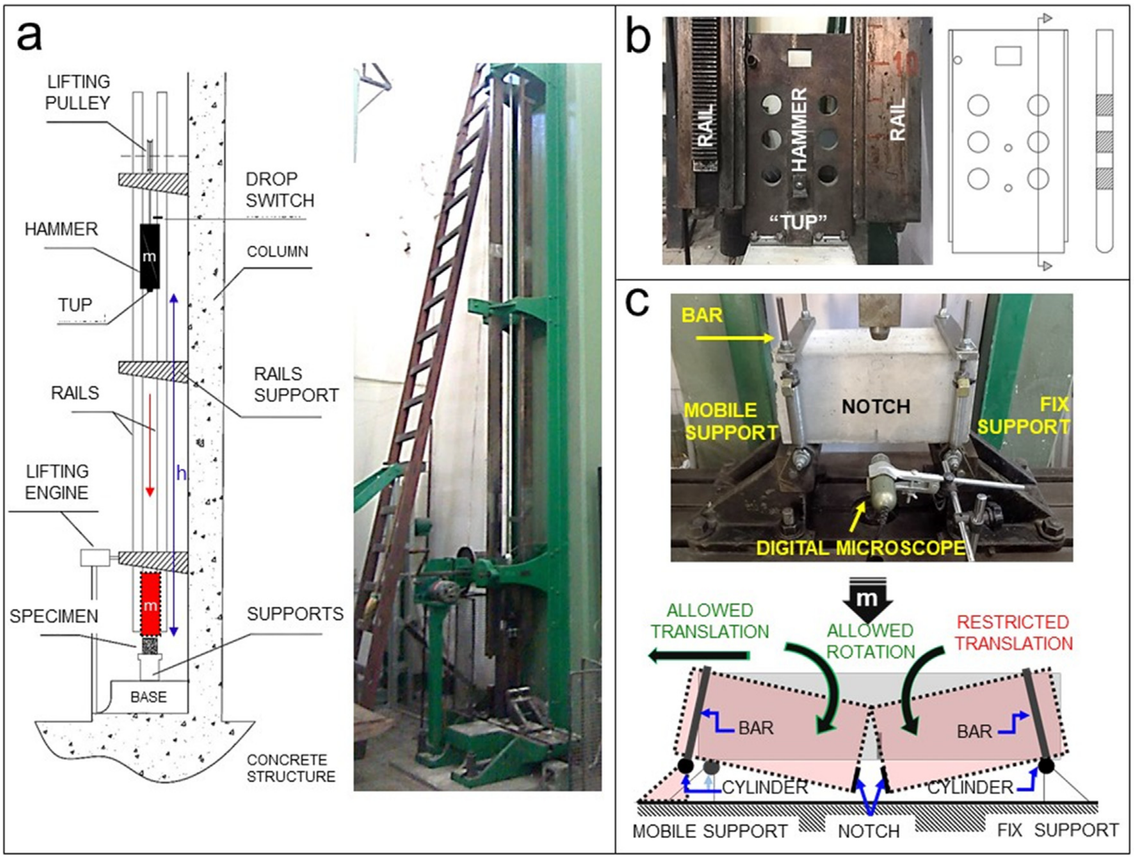

Fig. 3. a) Impact machine b) 5 kg Impact hammer c) Test setup.

Table 3
Impact test parameters.

Phase	m (kg)	h_0 (mm)	Δh (mm)	Number of drops	End	Properties
1	5	100	50	1	Visible crack (~20 μm)	E_C, COD_C
2			100	3	COD ≥ 3 mm	E_P, E_T, V_C
E_C: Energy at cracking COD_C: Initial Crack Opening	E_P: post cracking energy					
V_C: COD growth	E_T: Total Energy rate					

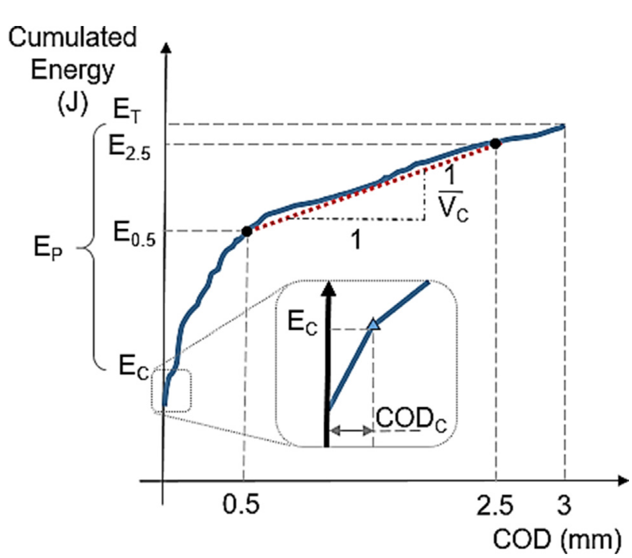

Fig. 4. Scheme of impact test curve. V_C = 2 mm / ($E_{2.5}$-$E_{0.5}$).

similar f_{R1} values) are given in Fig. 5. It can be seen that the curves are clearly different according to the type of reinforcement, consistent within the same group, with an acceptable variability in the post-cracking stage. Comparing the post-cracking response of FRC S25, P10 and G12, there are some differences in the shape of the curves. After the initial visible crack each FRC presents a different COD progress. In G12 it can be seen a first stage where it is necessary an important increment in energy to increase COD, this occurs for small crack opening. After that, a rapid growth of crack opening without major energy consumption takes place. In the case of S25, the COD gradually increases with the energy reaching a final energy similar to G12. A different response is showed by P10, which has both E_C and $E_{0.5}$ close to G12 and S25, but later its energy absorption capacity drastically increases. As expected, plain concrete (R) shows no increment in cumulated energy after cracking, as after few impacts the COD-limit is achieved. It must be noted that the failure was similar in all concretes, the crack starts at the notch and only deviates slightly from its plane.

Fig. 6 shows mean impact curves of each concrete and individual representative curves, where each symbol corresponds to one drop. A higher slope implies a lower COD growth rate (V_C).

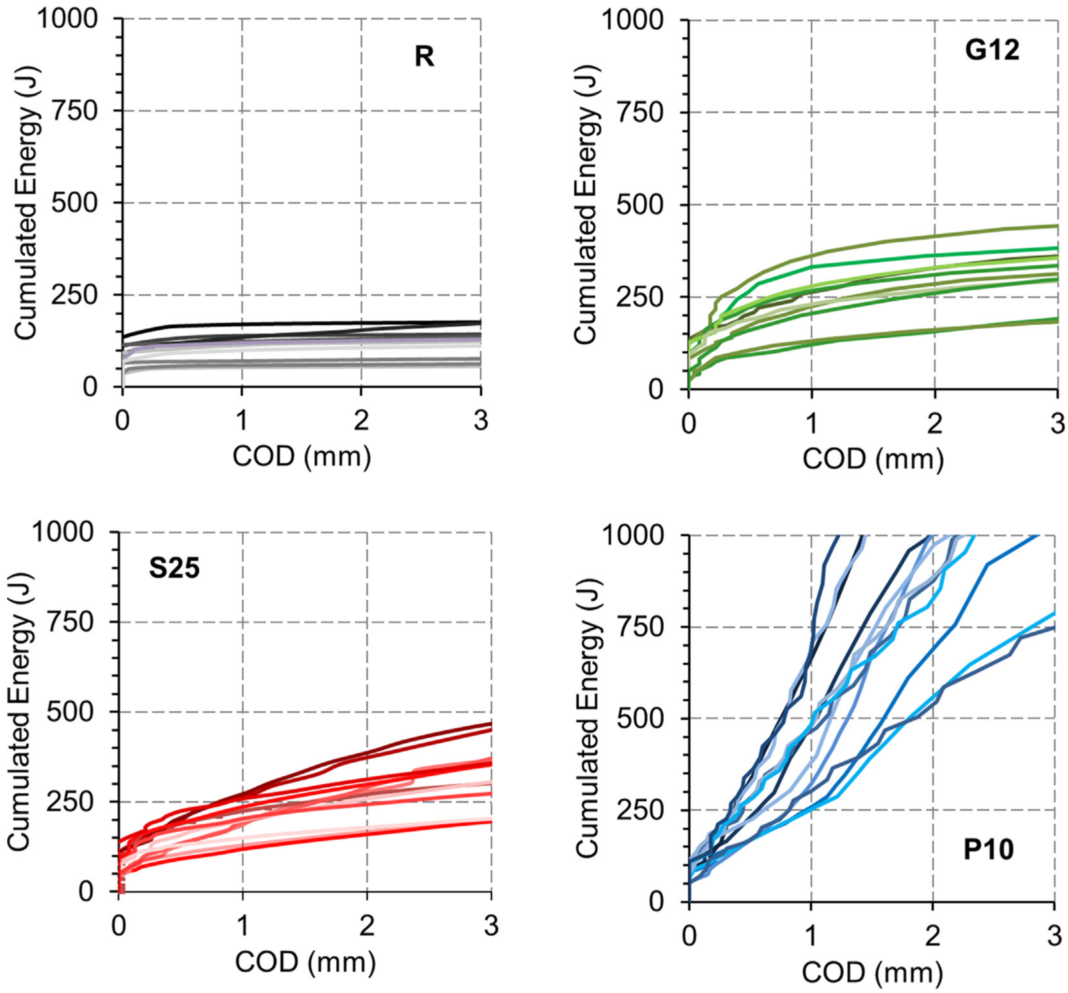

Fig. 5. Individual impact curves.

Table 4 gives the average, maximum and minimum values of the cracking, post-cracking and total energies (E_C, E_P, E_T). All concretes present similar E_C, indicating that it mainly depends on matrix strength; nevertheless, for each fibre type a very light E_C increase appears as the fibre content increase. Regarding the shape of the curves, it changes with the fibre type as different pull-out mechanisms developed. Steel FRC show a continuous growth of COD and a decrease in V_C as fibre dosage increases. In glass FRC the crack control capacity is lower than in concretes incorporating steel or polymer fibres, which is consistent with the static response in bending of these FRC. In addition, no significant differences in V_C between G6 and G12 were found. The particular response of poly-

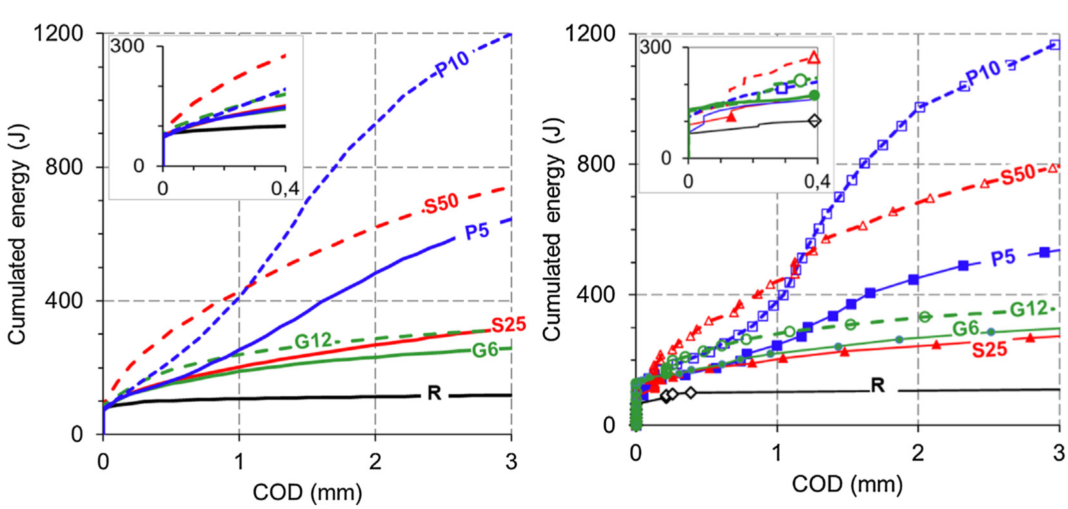

Fig. 6. (Left) Mean impact curve for each concrete. (Right) Individual typical curves where the symbols represent each impact.

Table 4
Impact test results.

Concrete	Fibres		Value	E_C	E_P	E_T	COD_C	V_C
	Type	(kg/m^3)		(J)			(μm)	(mm/J)
R	–	–	Mean	103	22	125	751	0.191
			Min.	48	5	176	46	0.102
			Max.	162	62	72	3660	0.393
S25	Steel	25	Mean	104	215	319	116	0.018
			Min.	50	111	459	43	0.009
			Max.	195	320	199	217	0.033
S50		50	Mean	111	670	780	69	0.007
			Min.	67	347	1698	1	0.002
			Max.	176	1525	414	174	0.012
G6	Glass	6	Mean	89	180	269	91	0.025
			Min.	52	80	391	43	0.013
			Max.	129	263	172	216	0.044
G12		12	Mean	114	221	334	111	0.019
			Min.	38	161	469	45	0.014
			Max.	167	318	198	217	0.030
P5	Polymeric	5	Mean	95	589	684	96	0.005
			Min.	54	386	1010	43	0.004
			Max.	123	955	473	174	0.008
P10		10	Mean	102	1183	1285	119	0.002
			Min.	65	698	1821	14	0.001
			Max.	136	1707	768	217	0.004

mer FRC is confirmed when analysing P5 and P10, after 1 mm a high increase in energy absorption capacity appears (very low V_C) and for COD exceeding 2 mm, the COD rate growth increases again.

The different responses clearly depend on the fibre type; they are significantly influenced by the bond mechanism and also by the number of fibres. In the cases of steel fibres the pull-out mechanism involves the deformation of the hook; in glass fibres debonding or breakage of filaments occur at relatively small openings; while polymeric fibres have high deformability, and this enables the progressive rupture of filaments, and consequently an increase in the energy absorption at large crack openings. As the filaments break in a progressive way, the fibre continues working; this phenomenon was more marked in P10 because the volume / number of fibres is very high. Fig. 7 shows the progressive breakage of a polymeric macrofibre, very close to the notch, as impacts are applied; each image includes the opening of the fissure (COD) and the corresponding number of impacts.

Fig. 8 compares the cracking and total energy of each concrete; the bars indicate the maximum and minimum values. In all cases the total energy increases with the fibre dosage. The lowest dispersion was found in G6 and the highest in S50. Contrary to the expected results in this case the variability, although dependent on the fibre type, did not decrease with the content of fibres, but even increased in some series. This can be associated with the distribution of fibres. The greater variability observed in concretes with higher energy, that required more impacts, could also be promoted by the low slenderness of the specimen. For this reason, and although the adopted specimen geometry is practical (easy to manipulate, it uses the same specimen as EN 14,651 [25] and is therefore suitable for FRC with fibers up to 60 mm length and aggregates up to 32 mm maximum size), new studies on the effect of the span/height ratio of the impact test results are in development.

Regarding the type of fibres, in the case of polymeric and steel fibres, the total energy clearly increases as fibre content increases.

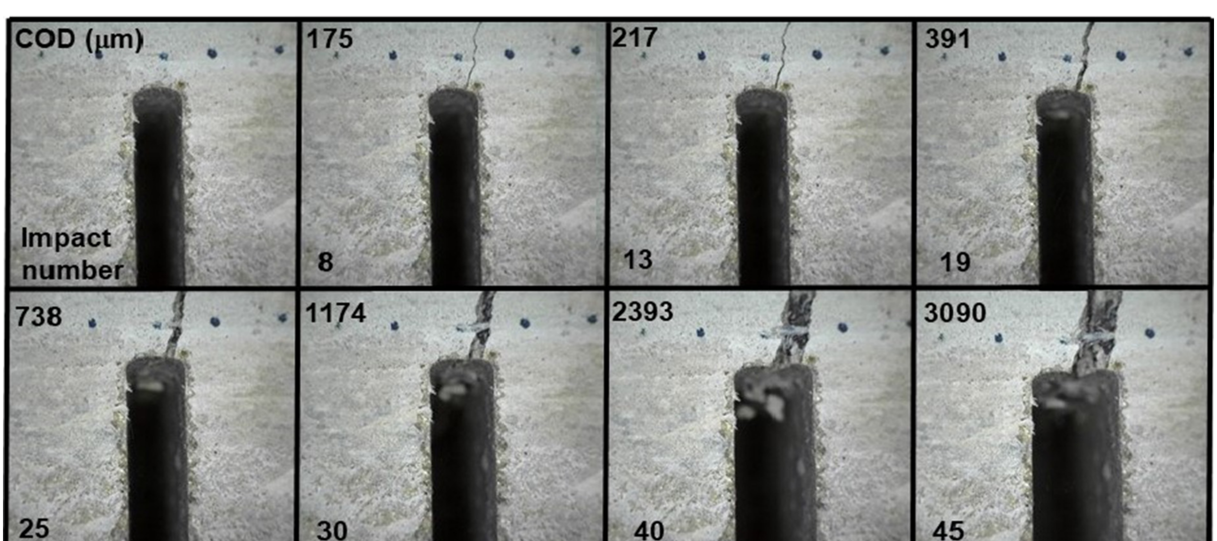

Fig. 7. Image sequence of development of the crack in a P10 specimen.

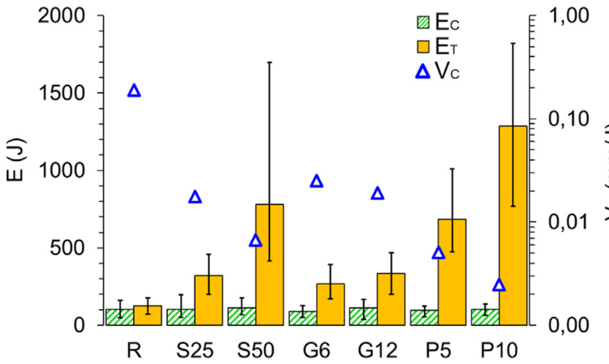

Fig. 8. Cumulated energy at cracking and after complete impact test.

On the contrary, although G12 has twice the content of fibres than G6, the post-cracking capacity was not substantially improved; this can be explained considering that as soon as matrix cracks fibres rupture takes place.

The initial visible crack opening (COD_C) of each concrete is also included in Table 4. It is confirmed that the fibre incorporation strongly reduces the initial crack size, even in the case of low toughness FRC. In concretes G and P the COD_C was greater for the higher dosages of fibres, and although this seems to be contradictory, can be justify as a greater impact energy was required to initiate cracking as can be seen when comparing the corresponding E_C values. On the contrary, in the case of steel fibres and although more energy was applied, the initial opening was smaller in S50 than in S25; this can be attributed to the elastic recovery capacity of steel FRC produced by the combined effect of the hook and the fibre stiffness. It must be mentioned that in plain concrete COD_C values can be very variable.

Table 4 and Fig. 8 also include the COD growth rate V_C (see Fig. 4) as it is an interesting tool for the analysis of concrete impact response. Both in steel and polymeric FRC V_C markedly decrease as the volume of fibres increases. On the contrary, glass FRC exhibited similar COD growth rates even though the content of fibres increases. (The values of V_C calculated for concrete R were included as a reference but it is evident that they are not useful for plain concrete characterization). The relationship between V_C and the residual parameters obtained in standard static tests will be discussed in the next section.

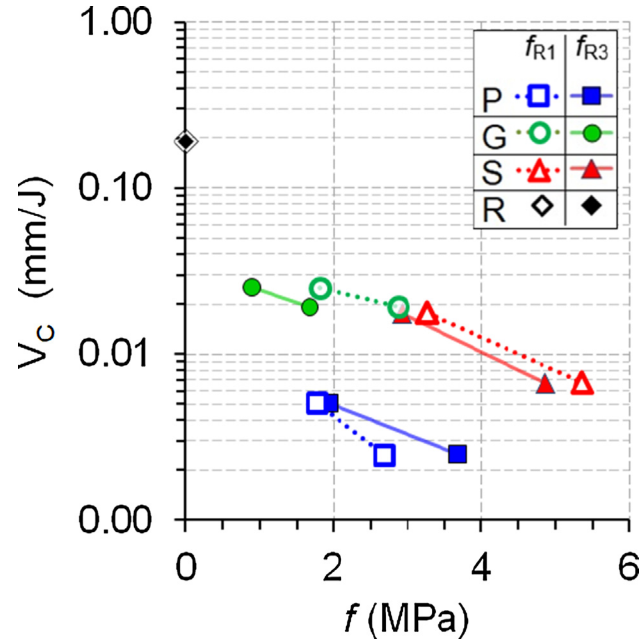

Fig. 10. Relationship between the COD growth rate and the static residual stresses in bending (EN 14651) [25].

4. Static response and impact resistance

Fig. 9 plots the relationship between the impact energy and the residual strengths used for FRC classification. The stresses f_{R1} and f_{R3} are representative of the FRC strength capacity at the serviceability limit state and at ultimate limit state respectively, as it is stated in the *fib* Model Code 2010 [24]. It can be seen that the total energy (E_T) increases as the residual stresses increase while the cracking energy (E_C) is practically independent of FRC toughness.

Fig. 10 shows the relationship between the COD growth rate and the residual stresses f_{R1} and f_{R3}; as expected, V_C decreases as FRC residual capacity increases, but the values depend on the fibre type, polymer FRC showed V_C results clearly lower. The mentioned dependence of the COD growth rate with the fibre type differs from what occurs in other conditions as, for instance, the control of cracks in conventionally reinforced concrete beams under static loading, where the contribution of fibres is mainly related to FRC toughness, regardless of fibre type and amount [30].

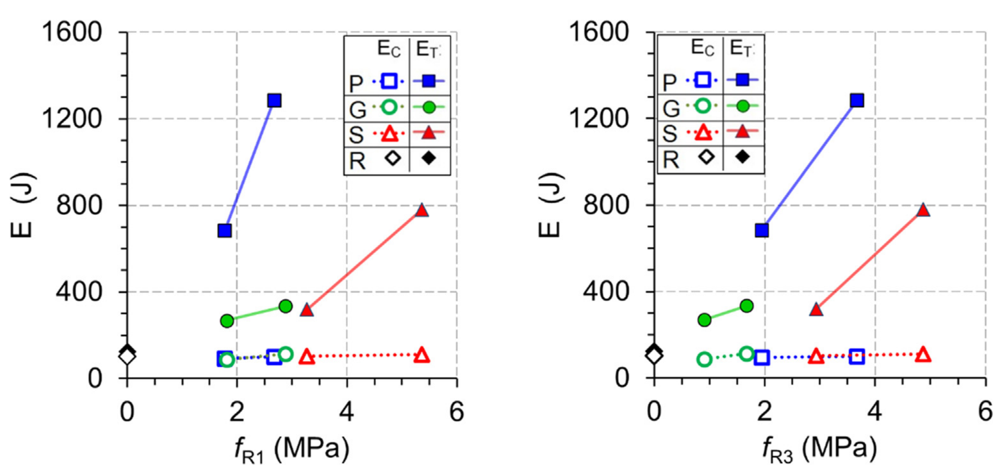

Fig. 9. Correlation between impact energy and static residual strength.

5. Conclusions

Although there are many different types of new fibres available for structural applications there is limited bibliography dealing with the impact behaviour of polymeric and glass ones. This paper presented the results of a study on the impact response of concretes incorporating steel, polymer and glass macrofibres. Both, the behaviour before and after cracking as well as the effect of the content of fibres were analysed. It was found that:

- The improvement of impact capacity produced by the incorporation of fibres depends on the type and content of fibres.
- Increments in concrete toughness, expressed as total energy applied during impact test, were mainly observed after matrix cracking, especially for steel and polymeric FRC.
- Steel fibres showed improvements both at cracking (smaller residual crack size) and during the post-cracking. Concrete reinforced with polymeric macrofibres were particularly efficient at large crack openings. The main contributions of glass macrofibres were at small crack openings.
- The variation of the cumulated energy with the crack opening differs according to the fibre type reflecting the different failure mechanisms involved.
- The concept of crack opening displacement growth rate can be used to evaluate the impact resistance of different FRC.
- A consistent correlation was found between the residual stresses in static bending and the measured impact parameters, but this relationship was not independent of the type of fibre.
- The implemented testing method was able to differentiate the impact performance, both before and after cracking, of concretes reinforced with different types of fibres. The adopted specimen geometry is practical, easy to handle and appropriate for all types of FRC, however further studies are required to optimize the test configuration.

CRediT authorship contribution statement

J.C. Vivas: Investigation, Methodology, Formal analysis, Writing - original draft, Writing - review & editing. **R. Zerbino:** Conceptualization, Supervision, Formal analysis, Funding acquisition, Methodology, Writing - review & editing. **M.C. Torrijos:** Investigation, Methodology, Formal analysis, Writing - review & editing. **G. Giaccio:** Conceptualization, Formal analysis, Funding acquisition, Methodology, Writing - review & editing.

Declaration of Competing Interest

The authors declare that they have no known competing financial interests or personal relationships that could have appeared to influence the work reported in this paper.

Acknowledgments

The authors specially thank the collaboration of Eng. Francisco Hours and Pablo Bossio on the support of the experimental works. Funding from LEMIT-CIC and from projects of National Scientific and Technical Research Council (CONICET) PIP112-201501-00861 *Advances in Fibre Reinforced Concretes*, and UNLP 11/I188 *Fibre reinforced concretes and other composites for the construction and repair of sustainable infrastructure*, is greatly appreciated.

References

[1] M. Drdlová, J. Buchar, J. Krátký, R. Řídký, Blast resistance characteristics of concrete with different types of fibre reinforcement, Struct. Concr. 16 (2015) 508–517, https://doi.org/10.1002/suco.201400080.
[2] B. Luccioni, F. Isla, R. Codina, D. Ambrosini, R. Zerbino, G. Giaccio, M.C. Torrijos, Experimental and numerical analysis of blast response of high strength fiber reinforced concrete slabs, Eng. Struct. 175 (2018) 113–122, https://doi.org/10.1016/j.engstruct.2018.08.016.
[3] B. Luccioni, F. Isla, R. Codina, D. Ambrosini, R. Zerbino, G. Giaccio, M.C. Torrijos, Effect of steel fibers on static and blast response of high strength concrete, Int. J. Impact Eng. 107 (2017) 23–37, https://doi.org/10.1016/j.ijimpeng.2017.04.027.
[4] M. Colombo, P. Martinelli, M. di Prisco, On the blast resistance of high performance tunnel segments, 2016. https://doi.org/10.1617/s11527-014-0480-7.
[5] T.H. Almusallam, N.A. Siddiqui, R.A. Iqbal, H. Abbas, Response of hybrid-fiber reinforced concrete slabs to hard projectile impact, Int. J. Impact Eng. 58 (2013) 17–30, https://doi.org/10.1016/j.ijimpeng.2013.02.005.
[6] G.A. Plizzari, S. Cangiano, N. Cere, Postpeak behavior of fiber-reinforced concrete under cyclic tensile loads, ACI Mater. J. 97 (2000) 182–192.
[7] J. Yahaghi, Z.C. Muda, S.B. Beddu, Impact resistance of oil palm shells concrete reinforced with polypropylene fibre, Constr. Build. Mater. 123 (2016) 394–403, https://doi.org/10.1016/j.conbuildmat.2016.07.026.
[8] X.C. Zhu, H. Zhu, H.R. Li, Drop-weight impact test on U-shape concrete specimens with statistical and regression analyses, Materials (Basel). 8 (2015) 5877–5890, https://doi.org/10.3390/ma8095281.
[9] T.D. Hrynyk, F.J. Vecchio, Behavior of steel fiber-reinforced concrete slabs under impact load, ACI Struct. J. 111 (2014) 1213–1224. https://doi.org/10.14359/51686923.
[10] N. Banthia, S. Mindess, J. Trottier, Impact resistance of steel fiber reinforced concrete, ACI Mater. J. 93 (1996) 472–479. https://doi.org/10.14359/9852.
[11] F.M. Mohee, The effects of strain rate on concrete strength under dynamic impact load, J. Bangladesh Electron. Soc. 16 (2016). https://doi.org/10.13140/RG.2.2.28749.08161.
[12] W. Radomski, Application of the rotating impact machine for testing fibre-reinforced concrete, Int. J. Cem. Compos. Light. Concr. 3 (1981).
[13] ACI Committee 544, Measurement of Properties of Fiber Reinforced Concrete 544.2R-89, 1999. http://civilwares.free.fr/ACI/MCP04/5442r_89.pdf.
[14] X.X. Zhang, G. Ruiz, R.C. Yu, A new drop weight impact machine for studying the fracture behaviour of structural concrete, WIT Trans. Built Environ. 98 (2008) 251–259, https://doi.org/10.2495/SU080251.
[15] P. Sukontasukkul, Impact behavior of concrete under multiaxial loading, The University of British Columbia, 2001.
[16] ACI Committee 544, Report on Measuring Mechanical Properties of Hardened Fiber Reinforced Concrete. ACI 544.9R-17, 2017.
[17] D.Y. Yoo, N. Banthia, Impact resistance of fiber-reinforced concrete – A review, Cem. Concr. Compos. 104 (2019), https://doi.org/10.1016/j.cemconcomp.2019.103389 103389.
[18] N.P. Banthia, S. Mindess, A. Bentur, Impact behaviour of concrete beams, Mater. Struct. 20 (1987) 293–302, https://doi.org/10.1007/BF02485926.
[19] V. Bindiganavile, N. Banthia, Polymer and steel fiber-reinforced cementitious composites under impact loading - Part 1: Bond-slip response, ACI Mater. J. 98 (2001) 10–16.
[20] V. Bindiganavile, N. Banthia, Polymer and steel fiber-reinforced cementitious composites under impact loading - Part 2: Flexural thoughness, ACI Mater. J. 98 (2001) 17–24.
[21] D.-Y. Yoo, S. Kim, Comparative pullout behavior of half-hooked and commercial steel fibers embedded in UHPC under static and impact loads, Cem. Concr. Compos. 97 (2019) 89–106, https://doi.org/10.1016/j.cemconcomp.2018.12.023.
[22] N. Doo-Yeol Yoo, Y.-S. Banthia, Impact resistance of ultra-high performance fiber-reinforced concrete with different steel fibers, 9th RILEM Int. Symp. Fiber Reinf. Concr. (2016) 398–405.
[23] T. Rahmani, B. Kiani, M. Shekarchi, A. Safari, Statistical and experimental analysis on the behavior of fiber reinforced concretes subjected to drop weight test, Constr. Build. Mater. 37 (2012) 360–369, https://doi.org/10.1016/j.conbuildmat.2012.07.068.
[24] International Federation for Structural Concrete (fib), Model Code Volume 1, (2012) 350.
[25] Technical Committee CEN/TC 229, EN 14651:2005 Test method for metallic fibered concrete - Measuring the flexural tensile strength (limit of proportionality (LOP), residual) Méthode, 2005. http://auber.com.vn/upload/download/445669281373.pdf (accessed April 17, 2018).
[26] American Society for Testing and Materials, ASTM C 39M:2003, Standard Test Method for Compressive Strength of Cylindrical Concrete Specimens, 2003.
[27] J. Vivas, R.L. Zerbino, Estudio de la resistencia al impacto de hormigones reforzados con fibras, in: 19° Congr. Int. Metal. y Mater. CONAMET-SAM, Valdivia, Chile, 2019: pp. 140–141.
[28] American Society for Testing and Materials, ASTM E436 – 03 Standard Test Method for Drop-Weight Tear Tests of Ferritic Steels, 1997. https://doi.org/10.1520/E0436-03R08.2.
[29] American Society for Testing and Materials, ASTM E208-17(2018) Standard Test Method for Conducting Drop-Weight Test to Determine Nil-Ductility Transition Temperature of Ferritic Steels, 2000. https://doi.org/10.1520/E0208-06R12.2.
[30] A. Conforti, R. Zerbino, G.A. Plizzari, Influence of steel, glass and polymer fibers on the cracking behavior of reinforced concrete beams under flexure, Struct. Concr. (2018) 1–11, https://doi.org/10.1002/suco.201800079.